Role of ice formation mechanisms occurring inside stylolite on limestone tilestone frost susceptibility

Yannick Igor Fogue Djombou, Philippe Devillers, Stéphane Corn, Eric Garcia-Diaz

Title: role of ice formation mechanisms occurring inside stylolite on limestone tilestone frost susceptibility

Authors: Yannick Igor Fogue Djombou[*,1,c], Philippe Devillers[2,b], Stéphane Corn[3,a], Eric Garcia-Diaz[4,a]

[*]Corresponding author
[1]yannick.fogue-djombou@univ-reunion.fr
[2]philippe.devillers@montpellier.archi.fr
[3]stephane.corn@mines-ales.fr
[4]eric.garcia-diaz@mines-ales.fr

[a]LMGC, IMT Mines Ales, Univ Montpellier, CNRS, Ales, France
[b]Laboratoire Innovation Formes Architecture Milieux, École Nationale Supérieure d'Architecture de Montpellier, 179 rue de l'Espérou, 34093, Montpellier CEDEX 5, France
[c]Consultant to the national association of Artisans Lauziers Couvreur in France and PIMENT laboratory associate researcher Reunion University

Highlight:

Low calorimetry measurement technics allow to determine stone frost features: freezing temperature and quantity of ice grown inside pores.

Presence of stylolite inside stone leads to increase locally the pore rate and size, with connected pores.

Stone frost damage is related to heterogeneous nucleation, followed by rapid growth and propagation of an ice front inside the connected porosity induced by stylolite.

Limestone tilestone without any stylolite and carrying a freezing temperature lower than the minimum of temperature often encountered in a region, will be frost resistant thus adapted for roofing in this region.

Increase of ice quantity inside stylolite pores comparing to host rock is a criterion to forecast stone frost susceptibility.

Abstract:

Freeze temperature and ice quantity formed inside porous media has been investigated on limestone tilestone samples by Differential Scanning Calorimetry (DSC) measurements. The aim was to determine the role of these stone frost features on limestone damage to Freeze-Thaw (FT) cycles, in relation to the presence of stylolite inside their structure. In fact, the presence of stylolite inside the structure leads to increase locally the pore rate and size, with connected pores. This implies a local increase of ice quantity formed at the surround of stylolite. Damage is thus associated to a heterogeneous nucleation, a rapid growth and ice-front propagation inside pores induced by the presence of stylolite. Specimens exhibiting an increase of quantity of ice formed inside their stylolite -- of more than 30% compared to host rock -- were damaged by freeze/thaw cycles. Furthermore, stones with freezing temperature lower than the minimum of FT cycles temperature are frost resistant. Finally, low-temperature calorimetry appears to be a practical and cheap method for quickly assessing frost limestone susceptibility. For example, this method can benefit some modest heritage constructions in UNESCO World Heritage site "Causse & Cevennes", made by craftsmen who need to quickly know the frost resistance of the stones they use.

Keywords:

Freeze-thaw; limestone roof tiles; low temperature calorimetry; ice formation mechanisms; stylolite

Introduction

Tilestone is a natural stone material used in various European heritage architectures such as ovens or cazelles in the "Causses and Cévennes" perimeter registered on the UNESCO World Heritage List (France); such as Trulli also registered on the UNESCO World Heritage List in Alberobello (Italy); such as Apethorpe Palace in Northamptonshire (United Kingdom); such as the "Brandas das Gêmeas" in Sistelo (Portugal) or "borda" in Aragonese Pyrenees region (Spain) also registered World Heritage List, as illustrated in Table 1.

Table 1. examples of European architectural heritage roofed with tilestone

Country	Illustration	Heritage
England		Apethorpe Palace in Northamptonshire (© Gallagher)
Italy		Trulli in Alberobello (registred in UNESCO World Heritage List) (©UNESCO)
Portugal		Brandas das Gêmea - Peneda-Gerês national parc - Sistelo (©Barroso)
Spain		Sheepfold in Ordesa Monte Perdido National Parc (registred in UNESCO World Heritage List) (@Caubet)
France		Cazelle in Lot department (©Fogue Djombou)

The various sedimentary diagenetic processes occurring on this material formation can lead to different types of diagenetic features inside their internal structure [1]. Stylolite (Fig. *1*) is a common, and probably the most frequent diagenetic feature encountered in this sedimentary material [2]. This diagenetic feature results from the phenomenon of pressure-solution [2]. Pressure-solution is the petrologic process wherein minerals dissolve as the result of pressure applied externally to them [3]. This process can start as shallow as 90 m during diagenesis in sedimentary basins [4] and still be active during highly metamorphic conditions [5].

Fig. 1 an example of stylolite [6]

Stylolites are rough surfaces of dissolution, lined by a thin layer of relatively insoluble particles, which are thought to accumulate while the more soluble major constituent of the rock (e.g. carbonate, quartz) dissolves away [3]. Stylolite is characterized by its morphology, its size or amplitude and its internal composition (Fig. 2).

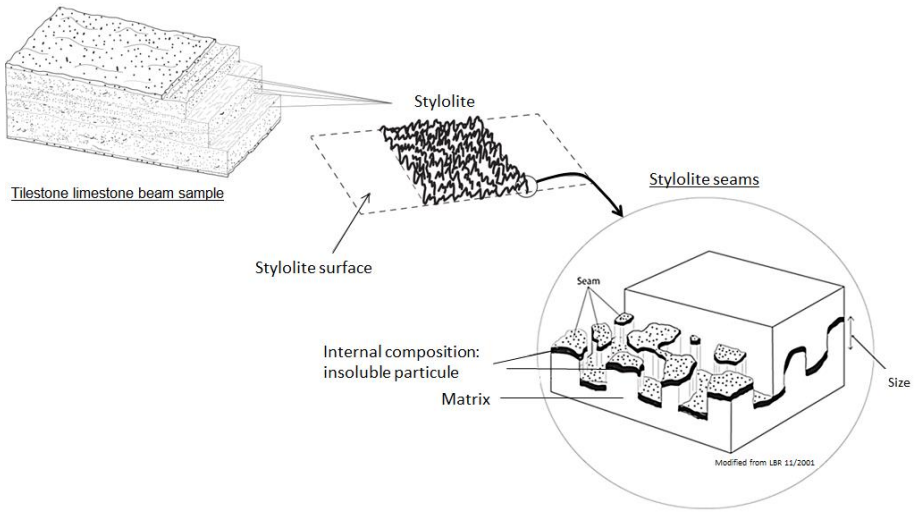

Fig. 2 Structure of limestone tilestone and stylolite [3]

Previous studies (Table 2) showed that this internal part of the stylolite implies a local increase of porous media than the host rock due to the transport of the soluble element after dissolution[7]. Thus, presence of stylolite may lead to an area of weakness where water could seep in. Turned into ice during freezing, it causes damages to tilestone [1, 8, 9]. Weathering processes occurring on stone subjected to freeze-thaw cycles were so far explained by the induced stresses related to ice growth mechanisms occurring in porous media [6, 7, 10–15]. In fact, the ice growth inside porous media can generate stresses due to hydraulic pressure caused by the crystal formed (Fig. 3).

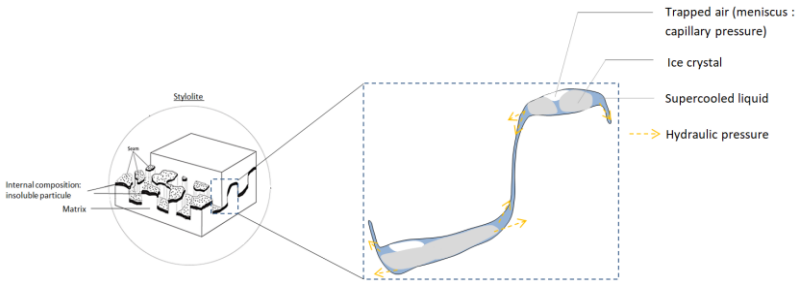

Fig. 3 Simplified representation of the pressure induced within the stylolite during freezing

In addition, the pore shape has an influence on the stresses developed. Indeed, if the ice crystal grows in a pore with a small radius entry, the stresses will be higher than if the crystals grown in pores with large entries because of a higher crystal-liquid interface curvature at the pore with small entry radius [14, 16] (Fig. 4). On tight sandstone, pore ice growing from larger pores into smaller ones, generate excess pressure that causes frost damage in micropores, which is manifested in the decrease in mechanical properties [14].

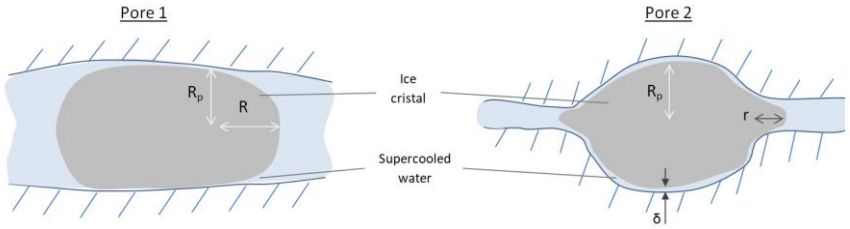

Fig. 4 Two pores shapes with different entry radii : pore 1 with large entry radius and pore 2 with small entry radius. Stresses induced during freezing are higher in pore 2 than pore 1 because of the high interface curvature (R>>r) [17, 18]

Pores shapes influence several stone physical parameters that control damaging mechanisms of stone subjected to FT cycles. For example, the degree of saturation beyond a certain threshold, between 70 and 80% [19, 20], could lead to damage. In addition, the rock texture influences the porous network structure which also plays a role in frost susceptibility. In this regard, oolithic limestones can carry inkbottle ooid voids served as expansion reservoirs that preserve stone during FT cycle [21]. Moreover, a grainstone with a bimodal porosity, a low degree of saturation and a high volume of trapped air is more resistant to frost than a mudstone facies which has an unimodal, well- connected pore network, a high degree of saturation and a low volume of trapped air [22].

Furthermore, in porous media, the appropriate temperature and pressure conditions for ice formation depend on the pore size (Fig. 5). In stone materials, it is often considered that, micropores correspond to pores with radius lower than 0,01µm, mesopores correspond to pores with pore radius range from 0,01 µm to 1 µm and macropores correspond to pores with pore radius upper to 1 µm [19, 23–25]. The temperature of crystallization inside these pores can range lower than -50°C [19–22]. For example, for a stone with micropore of 6 nm radius, water should freeze at -20° C [26].

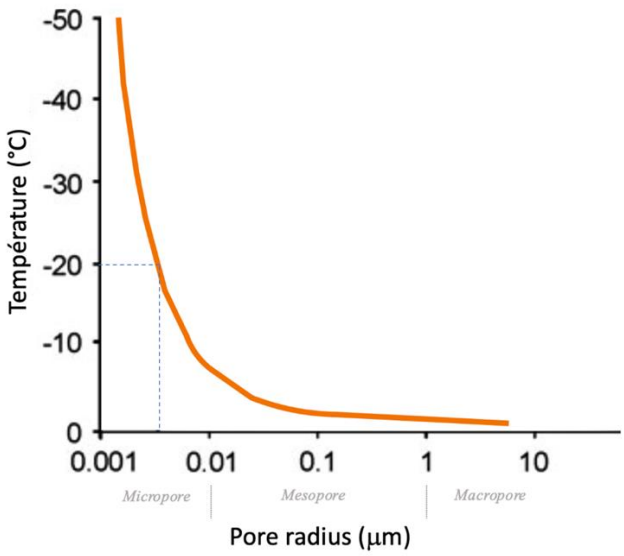

Fig. 5 Ice freezing temperature as a function of the radius of the pores after Stockhausen [26, 27]

The crystallization of ice is an exothermic reaction, which occurs in two stages: nucleation and crystal growth. The morphology of the pore network controls the phenomenon of nucleation and ice crystal growth inside the pore. Depending on the pore network characteristics (rate, size and connectivity), two mechanisms of ice formation can occur. The first is heterogeneous nucleation in macropores, followed by rapid growth and the propagation of an ice front. The second is homogeneous nucleation in unconnected pores, not allowing the propagation of an ice front. These mechanisms are well observed in the curve obtained from Differential Scanning Calorimetry (DSC) tests [28]. While the first mechanism is represented by a sharp peak in the heat flow curve, corresponding to an abrupt decrease in the heat flow, the second mechanism is represented by a more rounded curve [24] (Fig. *6*). Ice contented in porous media can be estimated by DSC measurements [29–31]. Finally, the minimum number of freeze-thaw cycles required to observe a clear deterioration of natural stones appears to be 50 cycles [26].

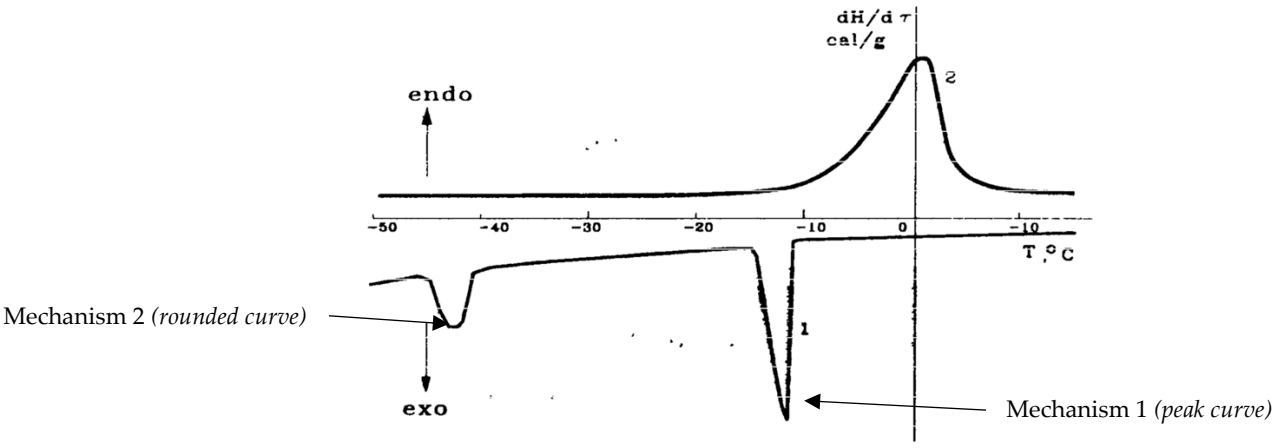

Fig. 6 Typical DSC-curve of freezing and thawing for cement stone. Mechanism 1 (peak curve): heterogeneous nucleation in capillary pores, followed by rapid growth and the propagation of an ice front, mechanism 2 (rounded curve): homogeneous nucleation in unconnected pores, not allowing the propagation of an ice front [28]

The degradation of the limestone roofing tiles subjected to freezing should likely be related to the freezing temperature and quantity of ice formed inside porous media, which has so far not been investigated. Thereby, the present work aims to use DSC measurement to examine the role of ice formation mechanisms on the damage process of limestone tilestone subjected to freeze-thaw cycles. After subjecting various samples, some with

stylolites, to different severe FT cycles, the influence of the quantity of ice formed in these diagenetic features on the frost susceptibility has been investigated. Finally, a criterion for predicting frost susceptibility, which relies on the assessment of the ice quantity formed inside the diagenetic features, is proposed. The finality of this study is to propose an alternative method, more affordable and more relevant, to assess quickly frost susceptibility of limestone tilestone.

Table 2 Table of relevant studies mentioned in this article

Title	**Authors**	**Journal and year of publication**	**Result**
Crystallization in pores	George W Scherer,	Cement and Concrete Research, 1999	For fracture to occur, the crystals must propagate through a region of the network large enough that the stress field can interact with the large flaws that control the strength
Physical deterioration of sedimentary rocks subjected to experimental freeze-thaw weathering	D.T. Nicholson, F.H. Nicholson	Earth Surf. Process. Landforms, 2000	Damage in limestone is due to pre-existing diagenetic features
Impact of stylolites on the mechanical strength of limestone	P. Baud, A. Rolland, M. Heap, T. Xu, M. Nicolé, T. Ferrand, T. Reuschlé, R. Toussaint, N. Conil	Tectonophysics, 2016	Presence of a stylolite lead to a significant strength reduction even if there are thin and closed
Kinetics of water freezing in mesopores determined by differential scanning calorimetry	Marcin Koniorczyk*, Piotr Konca	International Journal of Thermal Sciences, 2017	For a slow differential scanning calorimetry test, we could assume that ice grows much faster than temperature changes, therefore the equilibrium between ice and water exists at any temperature.
The permeability of stylolite-bearing limestone	Heap M, Reuschlé T, Baud P, et al	J Struct Geol, 2018	Stylolites are characterized by zone of higher porosity, with larger less spherical pores, than the host rock.
Freeze-thaw resistance of limestone roofing tiles assessed through impulse vibration monitoring and finite element modeling in relation to their microstructure	Y.I. Fogue Djombou, S. Corn, L. Clerc, D. Salze, E. Garcia-Diaz	Construction and Building Materials, 2019	The damage in limestone under freeze-thaw cycle is due to the pre-existing diagenetic features, such as stylolite, in its structure
Frost Damage in Tight Sandstone: Experimental Evaluation and Interpretation of Damage Mechanisms	Ding S, Jia H, Zi F, et al	Materials, 2020	Pore ice grows from larger pores into smaller ones, generate excess pressure that causes frost damage in micropores and then nanopores

1. Materials and Methods

1.1. Materials

1.1.1. Studied stones description

Limestone tilestone samples were taken from three active quarries at Montdardier, Laval-du-Tarn and Sauclière, located in the Gard, Lozère and Aveyron departments (in the southern area of the "Massif Central" region in France). Beam-shaped samples, polished section and smalls fragments were sampled from each selected tilestone. Samples L, M and S are respectively referred to Laval-du-Tarn quarry, Montardier quarry, and Sauclière quarry. Number n corresponds to the stratum where the stone was sampled. The Table 3 below summarizes the description of samples chosen for the study.

Table 3 designation of samples used for the study

Locality	**Geological age**	**Stone designation**	**Number of samples**	**Beam-shaped samples designation Xn= X: stone, n : sample number**
Laval-du-Tarn	Upper Jurassic (Rauracian-Sequanian)	Stone L	10	L1, L2, L3, L4, L5, L6, L7, L8, L9, L10
Montdardier	Upper Oxfordian	Stone M	5	M1, M2, M9, M11, M13
Sauclière	Lotharingian	Stone S	9	S1, S2, S3, S4, S5, S6, S7, S8, S9

Stones L and M are micritic limestones [32] made of 97% of calcite and Stone S is grey dolomite with varying facies and sedimentary figures [33]. These stones were chosen because firstly they are mainly used in vernacular construction in central massif area and secondly because they carry inside their structure a wide variety of diagenetic features often observed in this sedimentary stone [1]. In fact, from optical microscope observations of polished sections of these stone specimens, it is possible to distinguish diagenetic features such as: Ds= diagenetic and metamorphic effect (D) with stylolites and pressure solution features (s); Dv= diagenetic and metamorphic effect (D) with mineral veins and healed fractures (v); Wb= weathering effects (W) with banding (b); Sl=primary depositional structure (S) with laminations (l); Lm= lithological variations (L) with variations in mineralogical composition (m); Lt= lithological variations (L) with truncated surface (t) F= fracture (F), weak incipient fractures (w). The sampling was performed so as to have the entire range of pre-existing diagenetic features mentioned on Table 4 above.

1.1.2. Porous characteristics of studied materials

On the purpose to characterize the porous media of studied stones, standard NF EN 1936, standard NF EN 13755 and standard NF EN 1925 were used to obtain water-open porosity, saturation rate after 48 hours and capillary water absorption. The mercury intrusion porosimetry was carried out in Micromeritics AutoPore IV 9500 Series Mercury Porosimeters to investigate the pore size distribution. A sorption isotherm of stones studied was carried out using the static gravimetric method with salts saturated solutions. These physical properties are mentioned in Table 5, Fig. 7 and Fig. 8 below.

Table 4 Pre-existing diagenetic features and samples associated (Eg L1 = sample n°1 of Laval-du-Tarn quarry)

Initial diagenetic feature	Samples	Diagenetic feature description	Example of illustration
Ds	L1, L2, L3, L4, L5, L6, L10, M1, M9, M11, M13, S1, S2, S3, S4, S6, S8	metamorphic and diagenetic effect with stylolites and pressure solution features	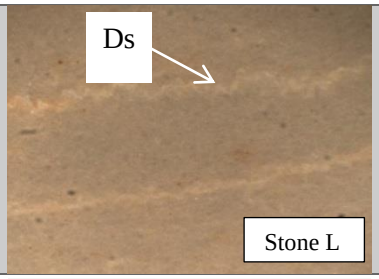
Dv	L1, L2, L3, L4, L5, L6, L7, L8	metamorphic and diagenetic effect with mineral veins and healed fractures	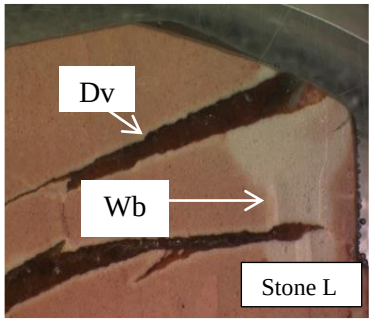
Wb	M1, M2, L1, L2, L3	weathering effects with banding	
Sl	S1, S2, S3, S4, S5, S6, S7, S8, S9	primary depositional structure with laminations	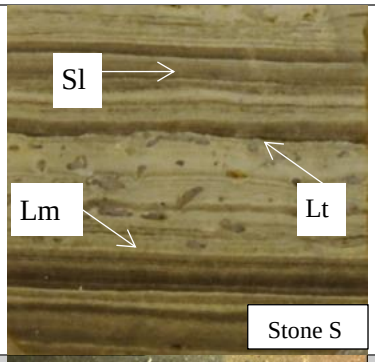
Lm	S1, S2, S3, S4	lithological variations with variations in mineralogical composition	
Lt	S1, S2, S3, S4	lithological variations with truncated surface	
Fw	M1, M2	Weak incipient fractures	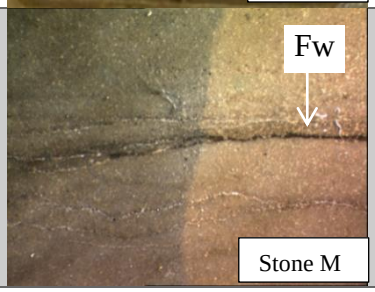

Table 5 physical characteristics of studied samples

	Stone L	*Stone M*	*Stone S*
Water-open porosity (%)	1.8	1.8	10.8
Apparent density (kg/m³)	2647	2630	2513
Saturated porosity at 48h (%)	1.5	1.7	9.1
S48 water-saturation coefficient (%)	80	95	85
Absorption coefficient (g/cm²/√s)	2.3	30.2	0.4
Mercury intrusion porosity (%)	0.9	-	7.4
Average pore diameter (nm)	15	-	143

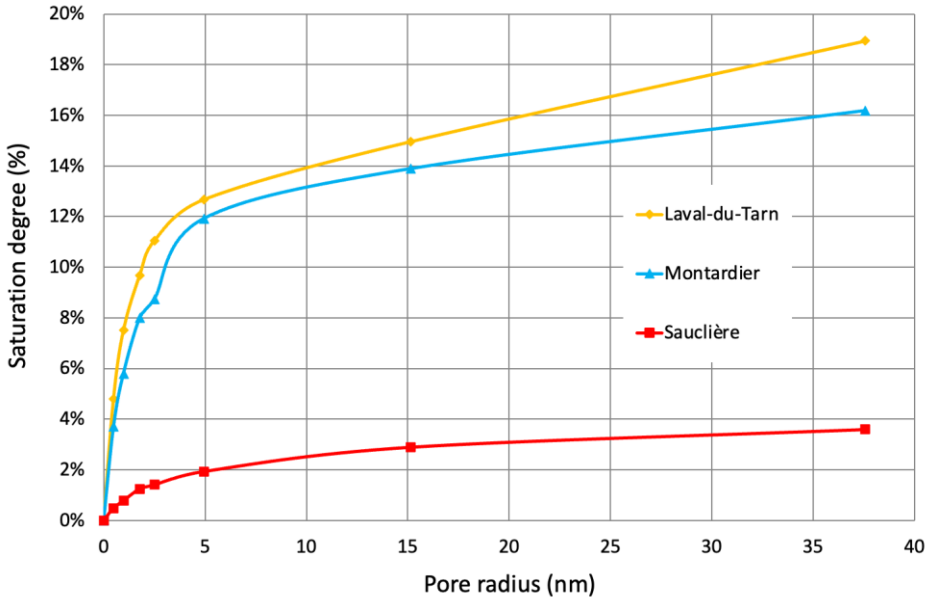

Fig. 7 Results of sorption isotherm

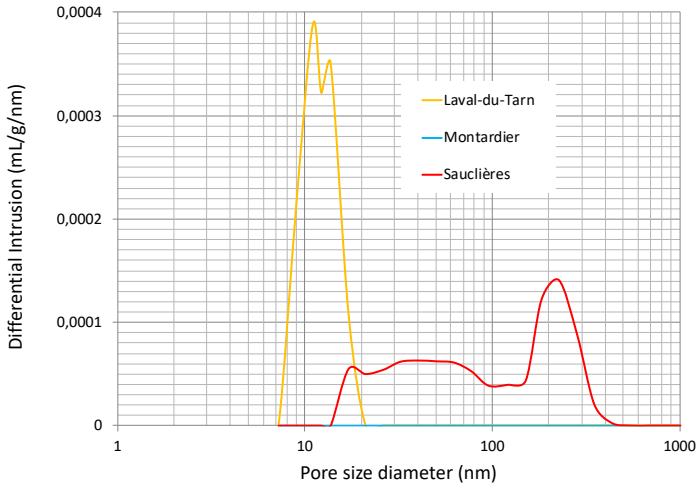

Fig. 8 Pore size distribution curves of the studied limestones obtained by mercury intrusion measure

The results from the porous characterization of these materials present two categories of rock. A first with a mudstone facies with low porosity and high rate of micropore of radius under 10 nm, and second category of rock with bimodal connected micropore distribution, with high rate of micropore radius over 100 nm. Although the stone M has the same pore characteristics of stone L (according to capillary water absorption and water-open porosity measurement, …), it did not present any signal to mercury intrusion porosimetry. This may be explained by the fact that the porosity of stone M is divided and is not accessible by mercury intrusion porosimetry which is useful for connected porosity. According to these porosity assets, except for stone S, stones L and M are likely frost resistant for common climate. In fact, they have ice freezing temperature under common temperature, so ice does not form and there is no induced stress. This hypothesis will be investigated in this study.

1.1.3. **MEB stylolite observation**

For each stone, stylolites have been observed, on pieces of cylindrical polished samples of 3 cm of diameter with the Quanta 200 FEG SEM from FEI coupled to an Oxford INCA X-sight energy dispersive X-ray spectroscopy (EDX) analyzer (Fig. 9).

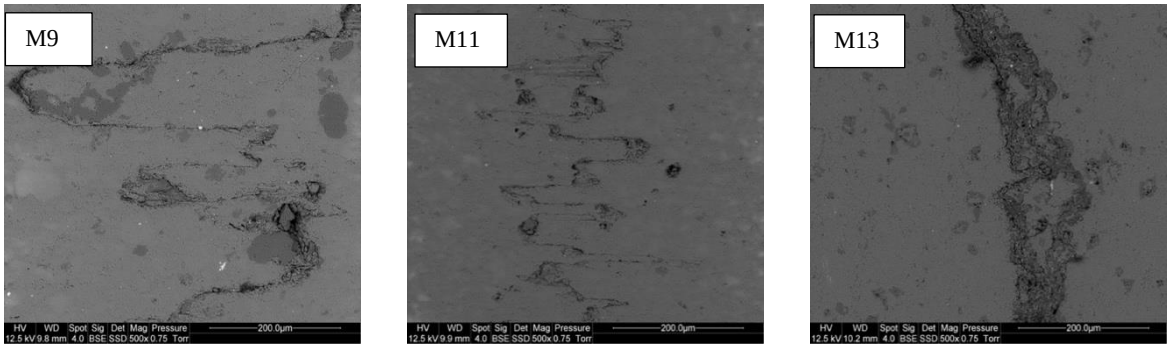

Fig. 9 SEM observation of different size of stylolite on Montardier rock.

To characterize the severity of diagenetic flaw, we evaluated the porosity increased locally, by comparing the local porosity, obtained by image analysis, with the total porosity of the stone. Gray-level threshold analysis, with ImageJ software, allows to determine the local porosity. Then flaw severity is obtained by dividing total porosity to imageJ local porosity. According to this measure, M9 and M13 have the highest flaw severity. It is not possible to characterize stylolite of sample S4, because host rock porosity is high and cannot be distinguished at gray-level image to the stylolite-induced porosity (Table *6*).

Table 6 stylolite characterization with ImageJ software threshold gray-level analysis

Sample name	Image J gray level analysis	Total porosity (%)	ImageJ local porosity (%)	Flaw severity
Sample L1	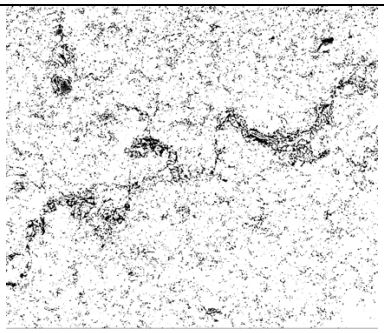	2,9	9,23	3,18
Sample M9	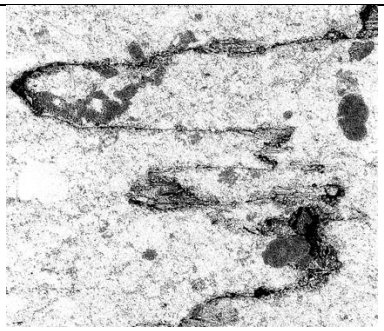	3,44	22,53	6,55
Sample M11	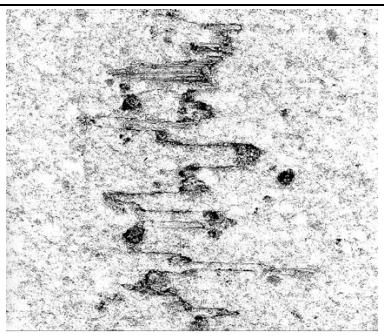	3,44	16,71	4,86
Sample M13	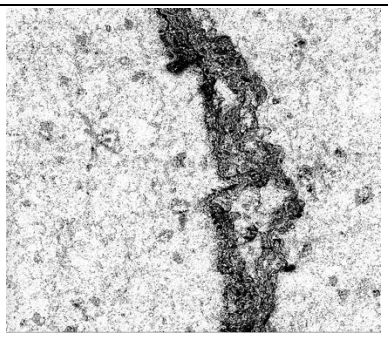	3,44	23,13	6,72
Sample S4	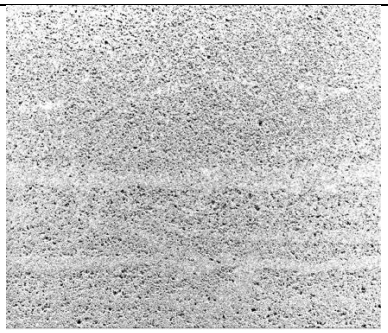	11,99	23,42	1,95

1.2. Methods performed.

On the purpose to characterize the damage occurred during the cycling tests and the role of stone frost features, multi-scaled investigations were carried out on samples (Fig. 10). Materials properties investigated are presented below:

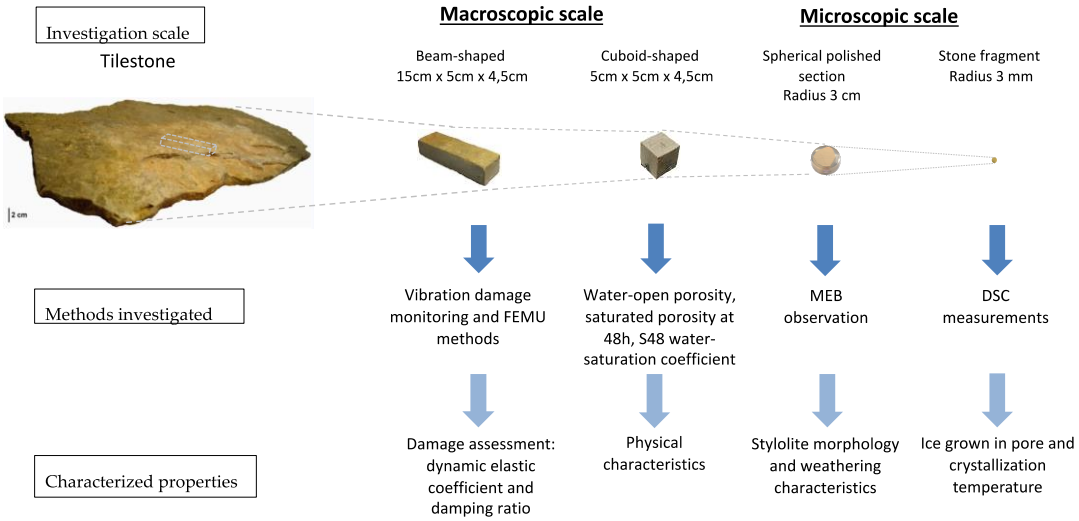

Fig. 10 multi-scaled methods investigated and characterized properties

1.2.1. Determination of stone frost features: freezing temperature and quantity of ice grown inside pores

In order to assess the freezing temperature of the water within the pores of stones, specimens were tested by Differential Scanning Calorimetry (DSC) over a temperature range from −30° C to 20° C, with a scanning rate of 10° C per minute. Before the tests, all the samples were saturated by immersing them for 48 hours at 20°C. The data obtained from Differential Scanning Calorimetry (DSC) measurements were analyzed with the software of the Pyris device so as to obtain the phase change temperatures T_{cryst} and the energy released ΔH_{cryst} during the phase change. The energy released during the fusion or crystallization of water corresponds to the area between the curve and the asymptote at the base of the curve.

The enthalpy of phase change ΔH_{ice} at temperature T is given by the formula from Matala [29], equation (1):

$$\Delta H_{ice} = 334+4.83T+0.0125T^2 \quad (1)$$

So the ice quantity χ (in g / g) formed during freeze inside the pores, is determined by the equation (2) below:

$$\chi = \frac{\Delta H_{cryst}}{\Delta H_{ice}} \quad (2)$$

In this article, we refer to stone frost features, both parameters freezing temperature and quantity of ice grown inside pores.

1.2.2. Mechanical damage monitoring and Finite Element Model Updating (FEMU) methods.

Vibration damage monitoring (VDM) and Finite Element Model Updating (FEMU) methods were performed to assess damages occurring during freeze-thaw test [9, 34, 35]. Modal parameters (natural frequencies) of the three first modes (two bends (one in the longitudinal axis and the other in the transverse axis) and one twist around the longitudinal axis) are determined with VDM methods. From

FEMU methods, it will be possible to obtain dynamic elasticity modulus by adjustment to an isotropic FEM. The FEMU method developed in this study, represented in the figure (Fig. 11), consists of minimizing the quadratic difference between the frequencies obtained experimentally and those obtained numerically by updating the elastic parameters of a finite element model. The minimization procedure was developed in the COMSOL software programming environment.

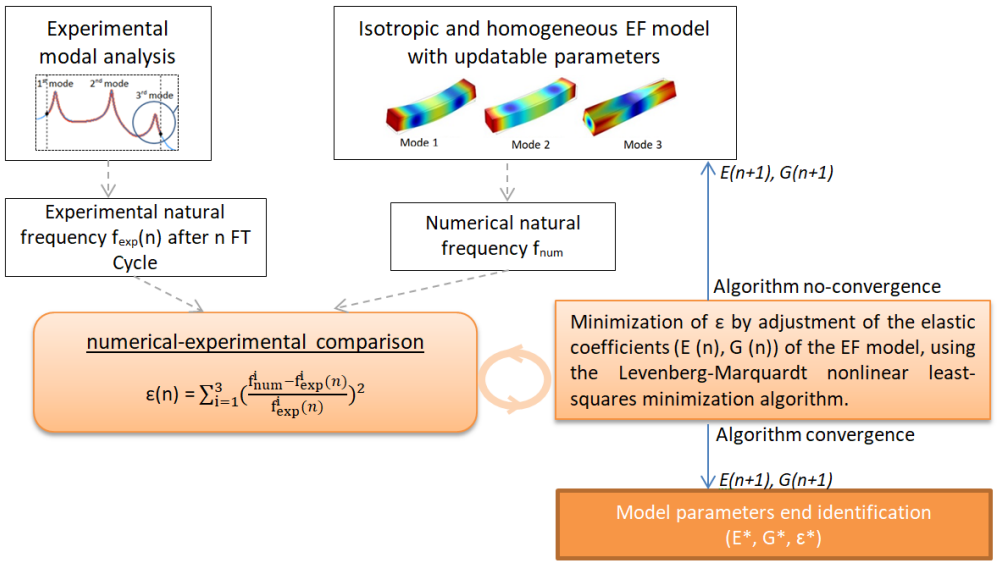

Fig. 11 FEMU procedure developed

Therefore, the loss of stiffness with the Relative Dynamic Elastic Modulus (RDEM(n)) obtained after every n cycles allow to assess the degradation occurring. The RDEM(n) are determined using the formulas below:

$$RDEM(n) = \frac{E(n)}{E(0)} \ (\%) \quad (3)$$

Where E(n) is dynamic elasticity modulus obtained after n cycles with FEMU method.

1.2.3. Freeze/thaw test setups

Several tests were performed on samples on the purpose to assess the frost resistance of studied stones. Freeze/thaw tests for this study were carried out in a Dycometal freezing chamber (model CHD - 525) (Fig. 13). Two freeze/thaw cycles, represented on Fig. 12 were performed:

- **Cycle FT1-FT4:** This test is divided in two parts: FT1 and FT4 cycles.
  Cycle FT1 was defined according to meteorological data for the studied geographical area, from the website infoclimat.fr. The data used for establishing the cycle are the hourly data for the period 1981-2010, from 5 weather stations: Gourdon (Lot), Mende-Brenoux (Lozère), Mende-Chabrits (Lozère), Millau-Soulobres (Aveyron), Rodez (Aveyron). Data analysis consisted in taking the days with the highest daily temperature amplitude and selecting those among them with the lowest temperatures (below -5 ° C). The test cycle developed from this analysis was in 4 parts: (1) decreases in temperature in chamber from 10°C to -12°C for 30min without water, (2) constant freezing temperature in chamber at -12°C for 1h30, (3) increase in temperature in the chamber from -12°C to 10°C for 30min, (4) constant thawing temperature in chamber at 10°C for 1h30 under water.
  Cycle FT4 was defined as the previous cycle, but making it even more severe by increasing the amplitude between the minimum and maximum temperatures, and it also consisted of four parts: (1) decreases in temperature in the chamber from 20°C to -30°C for 30min without water, (2) constant freezing temperature in the chamber at -30°C for 1h30, (3) increase in

temperature in the chamber from -30°C to 20°C for 30min, (4) constant thawing temperature in chamber at 20°C for 1h30 under water.
50 FT1 cycles follows by 50 FT4 cycles have been done.

- **Cycle FT3:** this test was performed so as to be harsher than the standard for natural stone (EN 12371) and consists in four parts: (1) decreases in temperature in chamber from 10°C to -30°C for 30min without water, (2) constant freezing temperature in chamber at -30°C for 1h30, (3) increase in temperature in the chamber from -30°C to 10°C for 30min, (4) constant thawing temperature in chamber at 10°C for 1h30 under water.
100 FT3 cycles has been done.

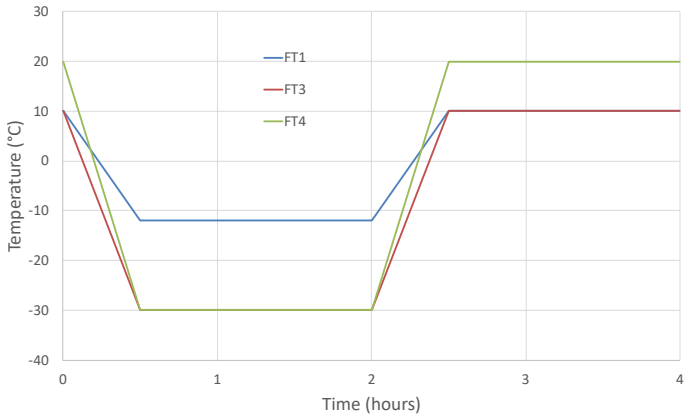

Fig. 12 the freeze/thaw experimental flow charts

Before beginning the cycles, all the samples (Table 7) were saturated by immersing them for 48 hours at 20°C. Thawing was done under water on the aim to keep the saturation degree constant in the sample.

Table 7 samples subjected to freeze/thaw cycle

Freeze/thaw cycle	**Sampled tested**
FT1 – FT4	L9, L10, L11, L12, L13, M9, M10, M11, M12, M13, S5, S6, S7, S8, S9
FT3	L1, L2, L3, L4, L5, L6, L7, L8, M1, M2, M3, M4, M5, M6, M7, M8, S1, S2, S3, S4

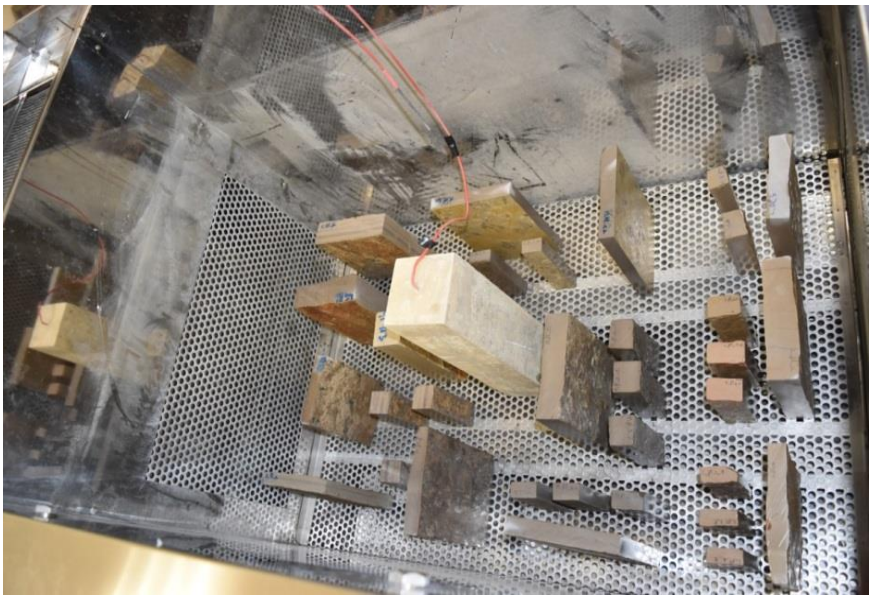

Fig. 13 Samples in the freeze/thaw chamber model CHD – 525

2. Results

2.1. Damages occurred during freeze/thaw cycles related to the diagenetic feature and the severity of the cycling test.

The first result of this study concerns the damage occurring in relationship with the test severity and the presence of diagenetic feature inside the samples. Damage was manifested by cracking apparition or high decrease of Relative Dynamic Elastic Modulus. A sample was considered as damaged if its RDEM decrease up 10%. In fact, all samples deteriorated, manifested by crack apparition, before the end of the FT cycles had an RDEM lower than 90%. Table 8, summarizes state of samples after 100 cycles.

Table 8 Comparison of damage-rate of samples after 100 FT cycles. Samples with stylolites are underlined

Damage after 100 cycles	FT1-FT4	*FT3*
No physical damages	L9, L10, L11, L12, L13, M10, M11, M12, S3, S5, S7, S9	*M3, M4, M5, M6, M7, M8, M2, L1, L2, L3, L5, L6, L7, L8*
Apparent crack or high (>10%) RDEM decrease	S6, M9, M13, S6, S8,	*L4, M1, M2, M17, S1, S2, S3, S4*

For convenient reading, we will present in following paragraphs results related to samples L1, M9, M11, M13 and S4 because they exhibited all degradation cases. For suitable comprehension, we propose the following graphic chart (Table 9)

Table 9 graphic chart use for results paragraph

	FT cycle	Denomination (italic for FT3 cycle and regular for FT1-FT4 cycle)	Line chart	Mark for sample with stylolite	Mark for sample without stylolite
Sample L1	*FT3*	*L1*			
Sample M9	FT1-FT4	M9			
Sample M11	FT1-FT4	M11			
Sample M13	FT1-FT4	M13			
Sample S4	*FT3*	*S4*			

Most samples carrying diagenetic features Ds (stylolite) or Fw (incipient fracture) were damaged during FT cycles. Furthermore, when the cycle is harsh -- low minimum temperature and high amplitude -- the damaging process occurred faster. For example, the cycle FT3 being harsher than first part (before 50 cycles) of FT1-FT4, *S4* was earlier damaged than M9 or M13.

However, for same cycling conditions, M13 sample presents earlier damage than M9 sample. This appears to be correlated to initial severity of the flaws inside the samples as the observations made with the SEM show.

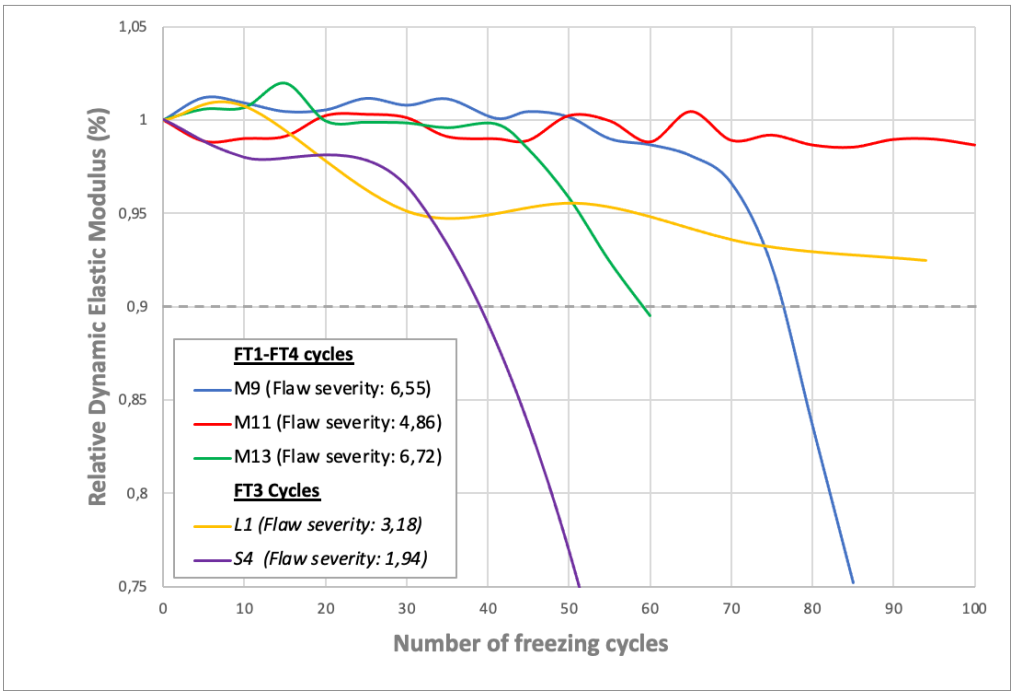

Fig. 14 Evolution of Relative Dynamics Modulus of Elasticity as a function of the number of FT cycles

Table 10 monitoring of Dynamics Modulus of Elasticity, RDEM and the number of FT cycle when the damaged occurred

	L1	**M9**	**M11**	**M13**	**S4**
Initial Dynamics Modulus of Elasticity (GPa)	58,8	67,9	59,3	58,2	60,2
Relative Dynamics Modulus of Elasticity after 50 FT1 cycles (%)	-	100,2	100,3	98,4	-

Number of FT3 cycles when damage occurred	>94	-	-	-	39
Relative Dynamics Modulus of Elasticity after 50 FT3 cycles (%)	95,5	-	-	-	73,8
Number of FT4 cycles after 50 FT1 cycles when damage occurred	-	30	>50	15	-
Relative Dynamics Modulus of Elasticity after 50 FT1 cycles + 50 FT4 cycles (%)	-	75,2	98,4	89,5	-

Thus, in this paragraph we confirm that limestone damage to FT cycles is related to the presence of pre-existing diagenetic flaws (stylolites) inside them and depends on initial severity flaw and the FT test harshness. The following results will concern further investigations on these diagenetic flaws.

2.2. Influence of stylolite on ice-growing mechanisms occurring inside its porous network during freezing

DSC measurements has been investigated on small Fragments from samples M9, M13, M11, L1 and S4. Fig. 15 represents normalized ENDO UP heat flow (W/g) for each specimen with stylolite (M9e, M11e, L1e, and S4e) and without stylolite (M9s, M11s, L1s, and S4s). The first observations made on these curves concerns their shapes. Some of them present a sharp peak (L1e, L1s, M9e, M13e, M13s, S4e and S4s) and other a rounded peak (M11s and M11e). Theses curve shapes correspond to the ice formation mechanisms occurring inside the pores. In fact, the first mechanism of ice formation, represented by a sharp peak, corresponds to heterogeneous nucleation in connected pores, associated to a rapid growth of ice-front propagation. The second mechanism, represented by a rounded peak, corresponds to homogeneous nucleation in segmented pores that do not allow the propagation of an ice front.

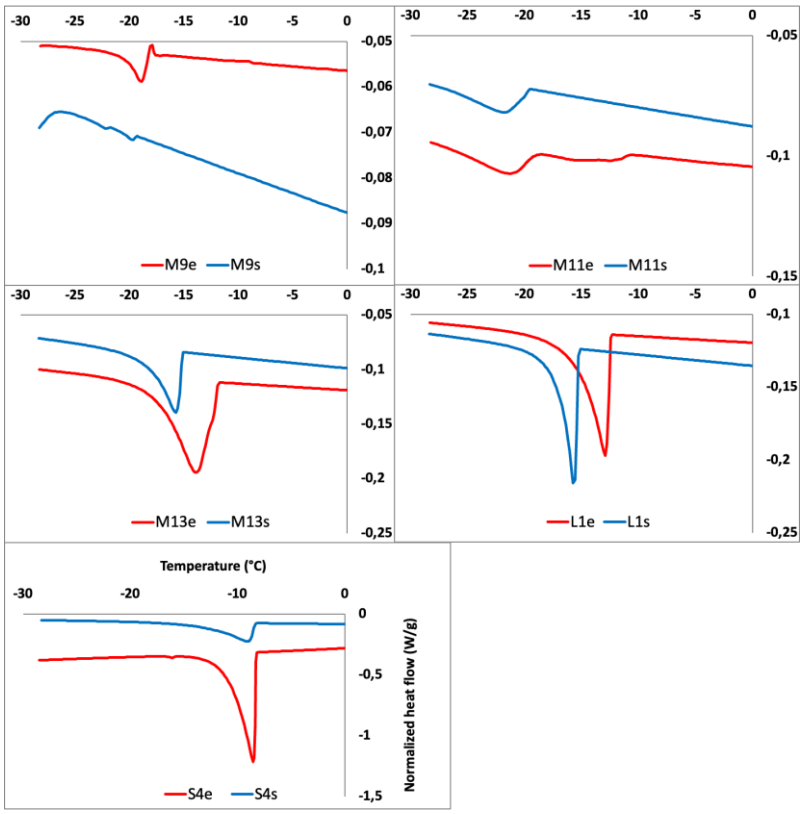

Fig. 15 example of comparison of normalized heat flow endo up between specimens with DS and specimen without DS

Samples deteriorated by freeze/thaw cycles present a heat flow curve with a sharp peak, and those that were not damaged present both sharp and rounded peak. So, the damage of the limestone is associated to mechanism of heterogeneous nucleation associated to a rapid growth of ice-front propagation inside stylolite pores. These mechanisms are controlled by stylolite pore assets. In fact, the presence of stylolite implies locally the increase of porosity rate and radius, and their connectivity. Following results will allow to verify these statements.

Table 11 Results summarize of comparison between mechanical damaging, flaw severity, ice formation mechanism and freezing temperature

	RDEM	Flaw severity	Ice formation mechanism	Freezing temperature with DS (°C)
Sample S4	*27,99%*	*1,95*	Heterogeneous nucleation followed by rapid growth and the propagation of an ice-front	-8,2
Sample L1	*92,48%*	*3,18*		- 12,6
Sample M9	75,20%	6,55	Homogeneous nucleation in segmented pores	-18,0
Sample M13	89,49%	6,72		-12,1
Sample M11	98,65%	4,86		- 18,8

2.3. Influence of stone frost feature on damaging in relation to pore and diagenetic features

The quantity of ice produced inside pores during freezing and the ice formation temperature (freezing temperature) have been determined. These parameters have been compared to the RDEM. Firstly, we observe that, the presence of stylolite influence stone frost features. In fact, two phenomena have been observed (Fig. 16). Firstly, the presence of stylolite leads to an increase of ice formation temperature. Secondly, the presence of stylolite causes an increase of the ice quantity formed inside stylolite pore comparing to host rock. These observations are consistent with the statement that stylolite can induced locally an increase of the rate and size of the pore than the host rock.

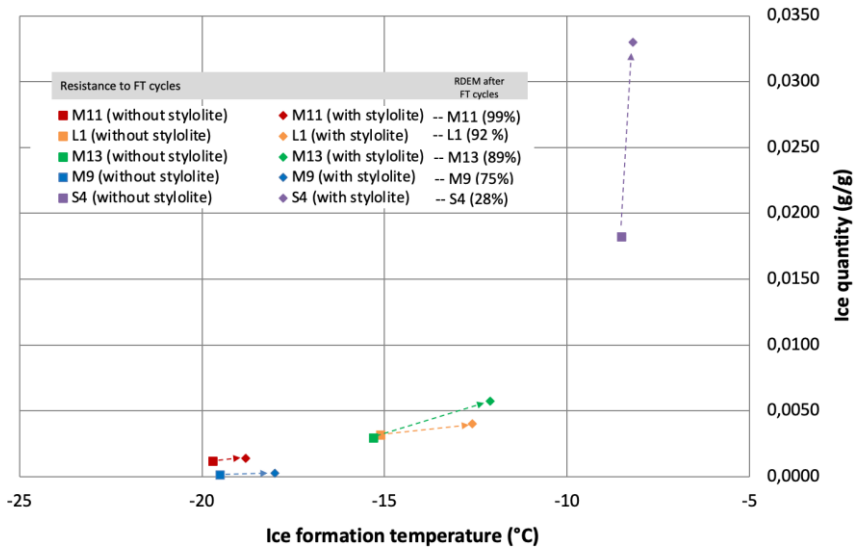

Fig. 16 Comparison of quantity of ice formed and ice formation temperature between samples with stylolites and samples without stylolites

None of the samples M9, M11, M13 were damaged after first 50 cycles of cycle FT1-FT4 (cf. Table 10 and Fig. 14). In fact, the FT1 minimum setpoint temperature (-12°C) is higher than the freezing temperature of samples M9 (-14,8°C), M11(-18,8°C), M13 (-12,1°C). When this setpoint become lower (-30°C) than the freezing temperature of stones, samples M9 and M13 were damaged and M11 resisted. These observations are consistent with the fact that if the freezing temperature of a stone is lower than the minimum temperature often encountered in a climate of a region, the stone will be frost resistant and adapted for roofing in this region.

The degradation of limestones does not necessarily depend on the amount of ice formed in the pores. In fact, samples S4, M9 and M13 have been damaged although the quantities of ice formed inside the pores are very different (Fig. 16). M9 and M13 damaged has very low ice quantity whereas S4 damaged has very high ice quantity. However, the amount of ice formed inside pores is consistent with the total porosity and pore size of the stones (Fig. 16). Although this ice quantity formed in M13 and L1 is very closed, L1 is frost resistant.

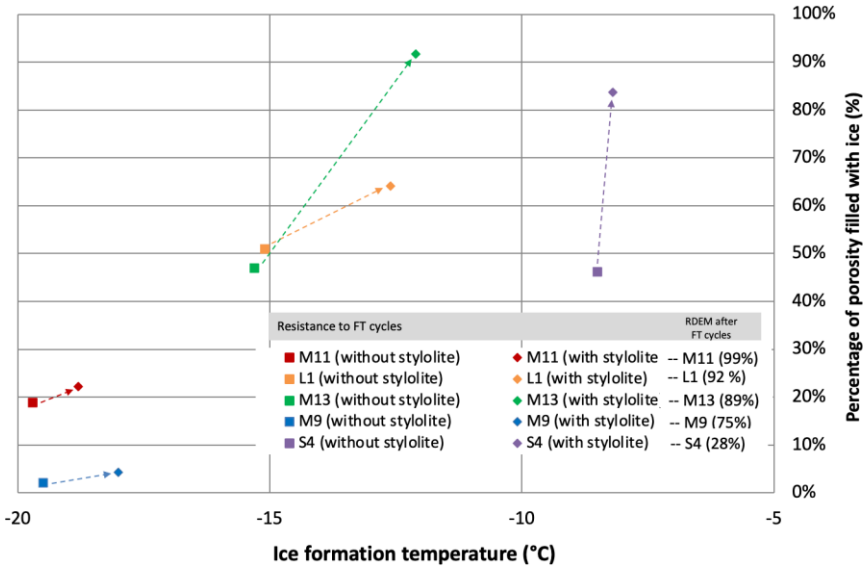

Fig. 17 Relation between percentage of porosity filled with ice and ice formation temperatrure

Concerning the percentage of pores filled with ice, damage can occur either when the percentage of porosity filled with ice is high (sample S4 and M13) or low (sample M9) (Fig. 17). However, sample M11 (frost resistant) exhibited a higher percentage of ice formed in the pores than sample M9 (frost damaged). Considering this, it is difficult to confirm the role of the percentage of porosity filled with ice on the frost deterioration of limestone. However, for stones with the same porous characteristics (sample M9, M11 and M13), the damage may be correlated with the flaw severity.

From observations made on this paragraph, it can be concluded that the measurement of the freezing temperature of a limestone without diagenetic flaws can allow to predict whether the material is adapted to a given climate. Insofar as if the freezing temperature of a stone is lower than the freezing temperature often encountered in a region, it will be frost resistant. The analysis of percentage of porosity filled with ice presents some intriguing results because the relation to damaging was not testified although the relationship between damaging and the stylolite flaw severity has been observed for a specific case -- stones with the same porous characteristics --.

2.4. Discussion: low-temperature calorimetry as a tool for assessing the frost susceptibility of limestone

On previous paragraph, we investigated the influence of stylolite presence inside a healthy host rock on frost damaging process. The presence of stylolite has the effect to increase locally the size and

the rate of the pore (Table *12*). However, we observed that the increase of pore size and quantity of ice formed in the pores is not enough to conclude on the frost susceptibility. In this paragraph, we will compare the quantity of ice formed in the rock with stylolite to the quantity of ice formed in the healthy host rock.

The increase of ice quantity formed in rock with stylolites is defined as follow:

$$I = \frac{\chi_s - \chi_h}{\chi_h} \quad (4)$$

Table 12 influence of stylolite on rock properties and ice formed quantity

	Freezing temperature in healthy rock (°C)	Freezing temperature in rock with stylolite (°C)	Ice quantity formed in healthy rock χ_h (g/g)	Ice quantity formed in rock with stylolite χ_s (g/g)	Increase of ice quantity	Damage rate (RDEM)
Sample S4	-8,5	-8,2	0,0182	0,0330	+81%	27,99%
Sample L1	-15,1	-12,6	0,0032	0,0040	+26%	92,48%
Sample M9	-19,5	-18,0	0,0001	0,0003	+112%	75,20%
Sample M11	-19,7	-18,8	0,0012	0,0014	+18%	98,65%
Sample M13	-15,3	-12,1	0,0029	0,0058	+95%	89,49%

Fig 18 shows the increase of ice quantity formed in stylolites in relation with RDEM. The observation of Fig. 17 shows a trend that when the increase of ice quantity formed in stylolites is higher, the damage severity is higher. According to the results of this study, a threshold of 30% may be defined: a tilestone limestone will be damaged by frost when the increase of ice quantity formed in stylolites is higher than 30%. Indeed, the pores of the stylolites are coarser than those of the host rock as shown by the SEM observations made (Fig. 9) as well as the results of the Table 12: the freezing temperature of healthy rock is systematically lower than that of rock with stylolites. The stylolites represent defects in the host rock in which will concentrate the degradations related to freeze-thaw cycles. In order to refine the critical threshold value, it would be necessary to carry out additional low temperature calorimetry tests on healthy rocks and on rocks with stylolites.

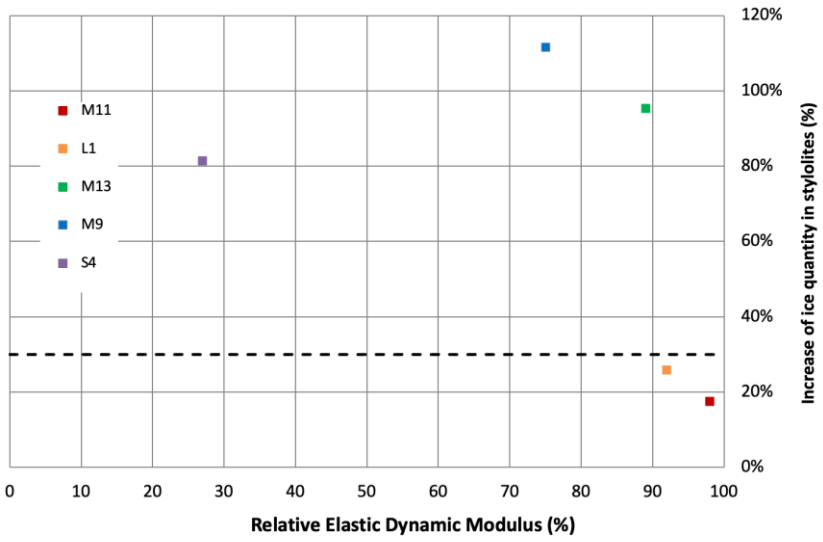

Fig. 18 Relation between increase of ice quantity inside stylolite and RDEM

3. Conclusions

The purpose of this study was to characterize the stone frost features and investigate their role on the damaging of freeze-thaw cycles, in relationship to the presence inside its structure of diagenetic flaw called stylolite. The first part of the study assessed the frost susceptibility of this material, using a vibration-based damage monitoring method in relation to the presence of stylolite inside the stone. The results confirm that damage is related to the presence of stylolite inside their structure, their severity, and the harshness of the test. Then, the stone frost features and their implication on damaging process were investigated. Firstly, for limestone rocks with a connected pores network (Laval-du-Tarn and Sauclière), it has been stated that degradation of these materials is associated to a mechanism of ice formation corresponding to heterogeneous nucleation, followed by a rapid growth and propagation of an ice front. For limestone rocks with a divided pores network (Montardier), it has been stated that degradation of these materials is associated to a mechanism of ice formation corresponding to homogeneous nucleation in unconnected pores. Besides, limestone tilestones without any diagenetic flaw and carrying a freeze temperature lower than the minimum temperature often encountered in a region, is frost resistant and suitable for roofing in this region. Finally, specimens that exhibited an increase in the ice quantity inside their stylolite of more than a threshold of 30% compared to their healthy matrix were damaged by FT cycles. It could be a criterion to forecast the frost susceptibility of the building material.

Subsequent studies will concern an investigation of low temperature calorimetry technics on more stone of various geology (schist, sandstone, …) so as to define a more precise frost susceptibility criterion based on frost features (freeze temperature and ice quantity growth). Thereby, in some construction projects, standard Freeze/thaw cycles, which are expensive, long, and tedious can be replaced by this criterium. For example, it could be helpful for certain modest heritage sites, where craftsmen need to quickly know if the rock taken in the surrounding can be used without problem for their construction project.

Funding

This research is a part of the project LAUBAMAC financed by “Commissariat Général à l’Egalité des Territoires” of the Massif Central in France.

Acknowledgements

The authors would like to acknowledge the quarries (Montdardier, SAS Lauzas, ALLA) for providing the samples that enabled us to conduct this study.

Data Availability Statement

The data that support the findings of this study are available from the corresponding author, upon reasonable request.

Bibliography

1. Nicholson DT, Nicholson FH (2000) Physical deterioration of sedimentary rocks subjected to experimental freeze-thaw weathering. Earth Surf Process Landf 25:1295–1307. https://doi.org/10.1002/1096-9837(200011)25:12<1295::AID-ESP138>3.0.CO;2-E
2. Flugel E (2004) Microfacies of Carbonate Rocks. Analysis, Interpretation and Application. Berlin, Heidelberg, New York: Springer-Verlag
3. L. Bruce Railsback (2001) An Atlas of Pressure Dissolution Features. http://www.gly.uga.edu/railsback/PDFintro1.html
4. Tada R, Siever R (1989) Pressure Solution during Diagenesis. Annu Rev Earth Planet Sci 17:89–118
5. Beach A (1979) Pressure solution as a metamorphic process in deformed terrigenous sedimentary rocks. Lithos 12:51–58

6. Toussaint R, Aharonov E, Koehn D, et al (2018) Stylolites: A review. J Struct Geol 114:163–195. https://doi.org/10.1016/j.jsg.2018.05.003
7. Heap M, Reuschlé T, Baud P, et al (2018) The permeability of stylolite-bearing limestone. J Struct Geol 116:81–93. https://doi.org/10.1016/j.jsg.2018.08.007
8. Baud P, Rolland A, Heap M, et al (2016) Impact of stylolites on the mechanical strength of limestone. Tectonophysics 690:4–20. https://doi.org/10.1016/j.tecto.2016.03.004
9. Fogue Djombou YI, Corn S, Clerc L, et al (2019) Freeze-thaw resistance of limestone roofing tiles assessed through impulse vibration monitoring and finite element modeling in relation to their microstructure. Constr Build Mater 205:656–667. https://doi.org/https://doi.org/10.1016/j.conbuildmat.2019.01.211
10. Ordóñez S, Fort R, Garcia del Cura MA (1997) Pore size distribution and the durability of a porous limestone. Quarterly Journal of Engineering Geology and Hydrogeology 30:221–230. https://doi.org/10.1144/GSL.QJEG.1997.030.P3.04
11. Deprez M, De Kock T, De Schutter G, Cnudde V (2020) A review on freeze-thaw action and weathering of rocks. Earth Sci Rev 203:103143. https://doi.org/10.1016/j.earscirev.2020.103143
12. Scherer GW INTERNAL STRESS AND CRACKING IN STONE AND MASONRY. In: Measuring, Monitoring and Modeling Concrete Properties. Springer Netherlands, Dordrecht, pp 633–641
13. Török Á, Szemerey-Kiss B (2019) Freeze-thaw durability of repair mortars and porous limestone: compatibility issues. Prog Earth Planet Sci 6:. https://doi.org/10.1186/s40645-019-0282-1
14. Ding S, Jia H, Zi F, et al (2020) Frost damage in tight sandstone: Experimental evaluation and interpretation of damage mechanisms. Materials 13:1–15. https://doi.org/10.3390/ma13204617
15. Benavente D, García del Cura MA, García-Guinea J, et al (2004) Role of pore structure in salt crystallisation in unsaturated porous stone. J Cryst Growth 260:532–544. https://doi.org/10.1016/j.jcrysgro.2003.09.004
16. Scherer GW (1999) Crystallization in pores. Cem Concr Res 29:1347–1358. https://doi.org/10.1016/S0008-8846(99)00002-2
17. Gilpin RR A model for prediction of ice lensing and frost heave in soils. Water Resour Res 16:918–930
18. Webber JBW, Dore JC, Strange JH, et al (2007) Plastic ice in confined geometry: the evidence from neutron diffraction and NMR relaxation. Journal of Physics: Condensed Matter 19:415117. https://doi.org/10.1088/0953-8984/19/41/415117
19. Prick A (1997) Critical Degree of saturation as a Threshold Moisture Level in Frost Weathering of Limestones. Permafr Periglac Process 8:91–99
20. Chen TC, Yeung MR, Mori N (2004) Effect of water saturation on deterioration of welded tuff due to freeze-thaw action. Cold Reg Sci Technol 38:127–136. https://doi.org/10.1016/j.coldregions.2003.10.001
21. Deprez M, De Kock T, De Schutter G, Cnudde V (2020) The role of ink-bottle pores in freeze-thaw damage of oolithic limestone. Constr Build Mater 246:118515. https://doi.org/10.1016/j.conbuildmat.2020.118515
22. Bellanger M, Homand F, Remy JM (1993) Water behavior in limestones as a function of pore structure: application to frost resistance of some lorraine limestones. Eng Geol 36:99–108
23. KUBELKA P (1932) No Zeitung für Elektrochemie
24. Peppin SSL, Style RW (2012) The physics of frost heave and ice-lens growth. Oxford
25. DEFAY R, PRIGOGINE I, BELLEMANS A, EVERETT DH (1966) Surface tension and absorption, Longmans e. London

26. Ruedrich J, Kirchner D, Siegesmund S (2011) Physical weathering of building stones induced by freeze-thaw action: A laboratory long-term study. Environ Earth Sci 63:1573–1586. https://doi.org/10.1007/s12665-010-0826-6
27. Stockhausen N (1981) Die Dilatation hochporöser Festkörper bei Wasseraufnahme und Eisbildung
28. Usherov-Marshak A, Sopov V (2002) Calorimetry of cement and concrete
29. Matala S (1995) Effects of carbonation on the pore structure of granulated blast furnace slag concrete. Helsinki University of Technology, Finlande
30. Sun Z, Scherer GW (2010) Pore size and shape in mortar by thermoporometry. Cem Concr Res 40:740–751. https://doi.org/10.1016/j.cemconres.2009.11.011
31. Johannesson B (2010) Dimensional and ice content changes of hardened concrete at different freezing and thawing temperatures. Cem Concr Compos 32:73–83. https://doi.org/10.1016/j.cemconcomp.2009.09.001
32. Bodeur Y (1994) The Upper Jurassic lithographic limestones of the Causse de Blandas-Montdardier (Languedoc, France) in their palaeostructural framework. GEOBIOS 16:219–225
33. SCIAU Jacques (2003) Dans les pas des Dinausaures des Causses : Inventaires des sites à empreintes. Association Paléontologique des Causses
34. Viala R, Placet V, Cogan S (2017) Détermination de propriétés constitutives de pièces à géométrie complexe en matériaux composites par méthode mixte numérique / expérimentale dynamique non-invasive. In: Journées Nationales sur les Composites 2017. 77455 Champs-sur-Marne, France
35. Corn S, Ienny P, Dupuy JS, Daridon L (2009) Identification des propriétés viscoélastique d'un PMMA par analyse vibratoire : comparaison entre différentes méthodes expérimentales. In: 19 ème Congrès Français de Mécanique. Marseille